

# Thick-film Piezoceramic Micro-generators

S.L. Kok, N.R. Harris and N.M. White

## 1. Introduction

Wireless sensor networks have recently become a popular area of active research as they offer the possibility for implementation within the our environment for monitoring physical conditions such as pressure, temperature, acceleration, vibration, and chemical substance present around us. The networks of these systems are built up from a large number of single unit sensor nodes.

A sensor node is generally small in physical size (typically a few cm<sup>3</sup> or smaller) and consist of a sensor, a transceiver, and supporting electronics. They are connected as a wireless network and are sometimes isolated and embedded in structures, which are not easily accessible. The lifespan of the sensor node is critically dependent upon the power source it contains. Instead of using a limited lifespan source, such as battery as the main power source, ambient energy scavenging offers an improved solution for providing power to miniature sensor nodes for an indefinite period of time. There are several possible mechanisms for ambient energy scavenging including solar, acoustic, thermoelectric, and mechanical vibration.

As low-level mechanical vibrations are present in many types of environment this is one possible energy source for harvesting. Basically there are three methods for mechanical vibration to electrical energy conversion: electromagnetic, electrostatic, and piezoelectric.

With the decrease in power requirements for Very Large Scale Integrated (VLSI) components for sensor nodes (in the range of a few tens to hundreds of microwatts), the application of piezoelectric materials as micro-generators for harvesting energy from ambient vibration is feasible and has advantages over other techniques in terms of their relatively simple fabrication and the capability for integration with other electronic components.

## 2. Piezoelectric Micro-generator Model

A piezoelectric material has the ability to produce electrical energy when a mechanical stress is applied on it. This occurs because the applied mechanical stress deforms the electric dipoles, which are orientated in the molecular structure as local charge separations. The deformation of electric dipoles creates charge and hence a current (or voltage across the sample). This phenomenon is known as the 'direct' piezoelectric effect. The 'converse' (or indirect) effect occurs when an applied electrical field causes the piezoelectric material to become deformed.

The direct and indirect piezoelectric effects of a material can be written in constitutive equations as,

$$\text{Direct piezoelectric effect: } \{D\} = [e]\{S\} + [\varepsilon^s]\{E\} \quad (1)$$

$$\text{Indirect Piezoelectric effect: } \{T\} = [\gamma^E]\{S\} - [e]^T \{E\} \quad (2)$$

Where  $\{D\}$  is electric displacement ( $C/m^2$ ) vector,  $\{E\}$  is electric field strength ( $N/C$ ) vector,  $\{T\}$  is stress ( $N/m^2$ ) vector,  $\{S\}$  is strain (dimensionless) vector,  $[e]$  and  $[e]^T$  are piezoelectric coupling coefficients ( $C/m^2$ ) matrix and the superscript  $T$ , denotes the transpose of the matrix,  $[\epsilon^S]$  and  $[\gamma^E]$  are the electric permittivity ( $C^2/Nm^2$ ) matrix at constant mechanical strain and the stiffness coefficient ( $N/m^2$ ) matrix at constant electric field strength respectively.

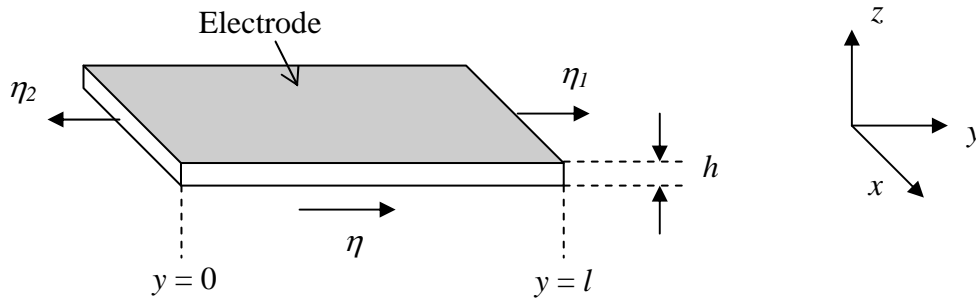


Fig.1. A piezoelectric rectangular plate vibrating in the longitudinal direction.

Fig.1 shows a rectangular plate of piezoelectric material with thickness  $h$ , width  $w$ , coated with electrodes on both the upper and lower surfaces of the material. When an a.c. voltage is applied on the electrodes of length  $l$ , the piezoelectric material will vibrate with displacements of  $\eta_1$  and  $\eta_2$  at the end of  $y = 0$  and  $y = l$ . (This assumes that the displacement of the material is only in the  $y$  direction and is rigidly clamped at  $y = 0$ ). The diagram of the electrical analogy of the mechanical vibrated piezoelectric material is shown in Fig.2 [1].

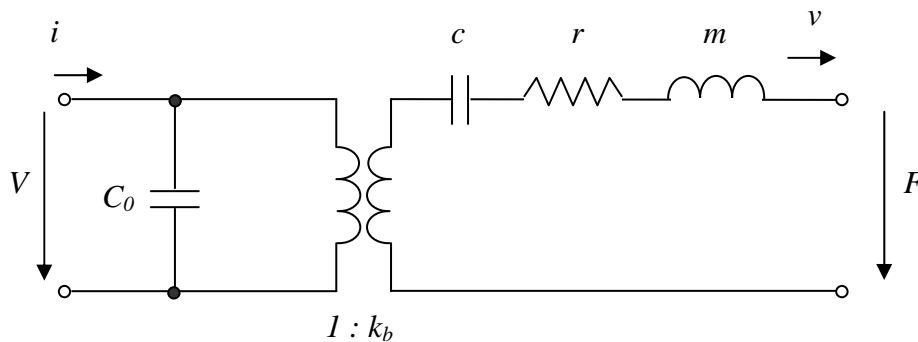


Fig.2. An electrical analogy of a mechanically vibrated piezoelectric material.

Where  $V$  is applied a.c. voltage,  $i$  is current flow in the circuit,  $F$  is force acting on cross section at  $y = l$ ,  $v$  is the velocity of the material at the cross section of  $y = l$ ,  $C_0$  is the static capacitance of the material,  $k_b$  is the conversion constant, the components of  $c$ ,  $r$  and  $m$  are derived from the mechanical impedance under vibration, representing the compliance, damping, and the mass of the material.

The mechanical part of the system at the right hand side of the analogous diagram in Fig.2, is similar to the general model of seismic energy conversion to electrical power, proposed by Williams and Yates [2] as shown in Fig.3.

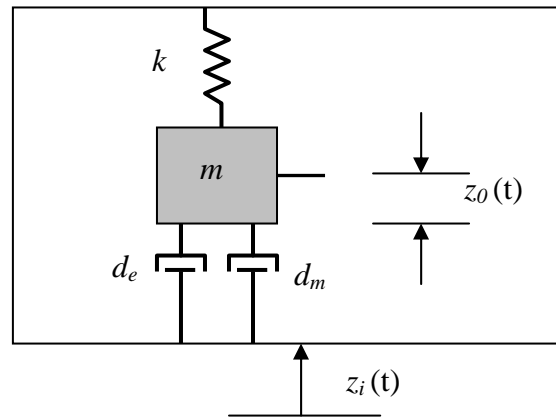


Fig.3. A vibration energy converter schematic diagram.  $k$  is the spring constant,  $d_e$  and  $d_m$  are the electrical and mechanical damping respectively,  $z_o$  is vertical displacement of the mass  $m$  from equilibrium, and  $z_i$  is the input amplitude.

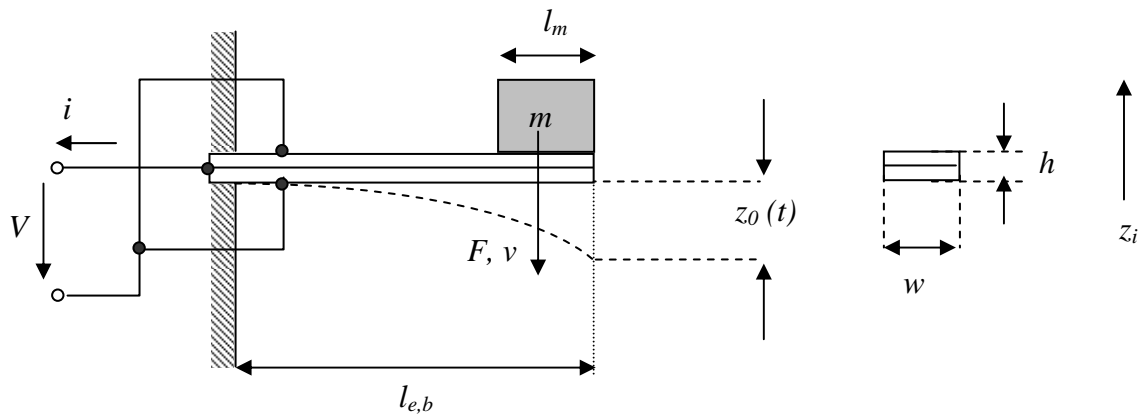


Fig.4. Schematic diagram of piezoelectric cantilever with proof mass  $m$ .

A piezoelectric micro-generator is often modelled as a rectangular cantilever beam, as shown in Fig.4, because it is easy to implement and effective for harvesting energy from ambient vibrations [3]. The natural frequency of a cantilever with total length  $l$ , thickness  $h$ , modulus of elasticity  $Y$ , and density,  $\rho$ , can be expressed as,

$$f_0 \propto \frac{h}{l^2} \sqrt{\frac{Y}{\rho}} \quad (3)$$

A dynamic model of a piezoelectric cantilever, developed by Roundy [4], suggests that the input stress, developed as a result of a mass flexing the beam, is equal to the sum of stress distributed in the system, i.e.,

$$T_{in} = T_m + T_d + T_Y + T_t \quad (4)$$

Where  $T_{in}$  is the input stress, proportional to the input vibration acceleration  $\ddot{z}_i$ ,  $T_m$  is stress due to inertial element, which is proportional to the induced acceleration of the beam  $\ddot{z}_0$ ,  $T_d$  is the energy dissipated because of damping elements,  $T_Y$  is the energy related to the structure elasticity function, and  $T_t$  is related to electric coupling of piezoelectric properties.

When the system is connected to an electrical resistance load  $R$ , and assuming that the driving frequency,  $\omega$  is matched to the resonance frequency  $\omega_0$  of the system, the output voltage is given by,

$$V = \frac{j \frac{2Yd_{31}h}{a\epsilon k_2} A}{-2\zeta\omega^2 + j \left( \omega^2 k_{31}^2 + \frac{2\zeta\omega}{RC_0} \right)} \quad (5)$$

Where  $j$  is the imaginary number,  $Y$  is the elastic constant for the piezoelectric material,  $d_{31}$  is the piezoelectric charge coefficient,  $a$  is the connection configuration of two piezoelectric layers (1 is for series and 2 is for parallel),  $\epsilon$  is the dielectric constant of the piezoelectric material,  $k_2$  is a constant related to the length of the beam  $l_b$ , electrode  $l_e$  and proof mass  $l_m$ ,  $A$  is the Laplace transform of the input vibrations in terms of acceleration,  $\zeta$  is damping ratio,  $k_{31}$  is piezoelectric coupling coefficient,  $C_0$  is the capacitance of the piezoelectric material.

The root mean square (rms) power is given as  $|V|^2/2R$ , therefore from equation (5), the rms power transferred to the resistive load can be written as,

$$P = \frac{1}{\omega^2} \frac{2RC_0^2 \left( \frac{Yd_{31}h}{a\epsilon k_2} \right)^2 A^2}{(4\zeta^2 + k_{31}^4)(RC_0\omega)^2 + 4\zeta k_{31}^2 (RC_0\omega) + 4\zeta^2} \quad (6)$$

### 3. Piezoelectric Materials for MEMS

There is a wide variety of different types of piezoelectric material. Some naturally exist in the form of crystals, such as Quartz, Rochelle salt, and Tourmaline group minerals. Others are polarised polycrystalline ceramics, such as barium titanate, and lead zirconate titanate (PZT). The final class is polymers piezoelectric materials such as polyvinylidene fluoride (PVDF) and polyimide, which can be manufactured and potentially integrated with MEMS [5].

Ceramics can be manufactured in the form of bulk material and films. Bulk piezoceramics are relatively large with a typical thickness exceeding 100  $\mu\text{m}$ . They are fabricated from a combination of ceramic materials and pressed at a high temperature (1100 – 1700 $^{\circ}\text{C}$ ) to form a solid poly-crystalline structure. The raw material used to fabricate bulk piezoelectrics is in powder form. The powder is then pressed and formed into components of the desired shapes and sizes, which are then mechanically strong and dense [6]. They are attractive for their good electromechanical properties (compared to other types of piezoelectric materials).

Piezoelectric charge coefficients,  $d_{31}$  and  $d_{33}$  are the properties commonly used to compare the performance of piezoelectric materials. As reported by manufacturers such as Ferroperm Piezoceramics [7] and Morgan Electroceramics [8], the piezoelectric coefficient,  $d_{33}$  for bulk materials can be in the range of 300 – 600 pC/N. One of the prominent applications of bulk piezoelectric material is to drive micro-fabricated mechanical amplifiers devices as reported in [9]. Bulk piezoceramics, however, tend to be relatively thick, which limit their application for micro-scale structures. Furthermore they need to be attached to certain parts of MEMS structures using mechanical or adhesive bonding, which is tedious and not cost effective. MEMS devices, which need piezoelectric structures with thickness of less than 100  $\mu\text{m}$ , are usually made from thin and thick film technologies, which can produce improved precision and finer structures.

Although piezoelectric polymer materials have relatively low piezoelectric strain constants (for example PVDF films have a measured  $d_{33}$  of only 24pC/N [10]), they do have much higher piezoelectric stress constants and low elastic stiffness, which give them advantages in producing high sensitivity sensors compared to tough bulk ceramic and brittle piezoceramics films. Piezoelectric polymers also have a high dielectric breakdown and operating field strengths, and can therefore withstand much higher driving fields than piezoceramics [11]. Their wide bandwidth, relatively low actuation power requirements and high generative force makes them popular for use in MEMS devices. However, for the applications in power generation, such as micro-generators, film technologies (particularly thick-films), can offer a better choice.

Piezoceramic films have some advantages over bulk and polymer piezoelectric materials. Although piezoceramic films do not have piezoelectric coefficients as high as bulk piezoceramics, for certain applications where a device thickness is required to be less than 100  $\mu\text{m}$ , film piezoceramics are more favourable for their fabrication compatibility with micro scale devices. Films can be deposited directly onto a substrate, using precise deposition techniques. They can be also processed at lower processing temperatures (800<sup>0</sup>C – 1000<sup>0</sup>C) than bulk ceramics.

Thin-film piezoelectric materials are compatible with MEMS processing technologies, but their electromechanical properties are much smaller than to bulk piezoceramics. Also they are not as flexible as thick-film materials, and although they are suitable for fabricating micro-sensors and micro-actuators, they are not the preferred choice for fabricating micro-generators. They require very high frequencies to operate as described by Jeon *et al* [12], where the thin-film device was capable of generating 1  $\mu\text{W}$  into a 5.2 M $\Omega$  resistive load at 13.9 kHz and with acceleration 250 m/s<sup>2</sup>.

Thick-film technology offers the possibility of producing piezoelectric microgenerators that can operate at lower vibration levels than those produced by thin-film techniques and are also compatible with MEMS technologies.

#### **4. Thick-film Piezoceramic**

Thick-film technology is traditionally used to manufacture a variety of resistor networks, hybrid integrated circuits and other electronic components [13]. In the past two decades, the research in thick-films has been extended to include sensing capabilities [14]. One of the early applications of thick-film sensors was in the area of strain gauge technology [15, 16].

Recently, the improvement of high piezoelectric activity in lead zirconate titanate (PZT) films, has brought thick-film technology to another level of development, where it is possible to fabricate micro-generators for embedded and remote systems [17]. The thick-film paste for fabricating micro-generators, however, is not commercially available and hence, has to be formulated in-house to suit to this purpose.

Typical piezoceramic thick-film fabrication steps are conducted in sequence starting from paste composition, screen-printing deposition, drying and co-firing and finally polarisation of the film. Some of the main issues for piezoelectric thick-film fabrication involve the production of films that are uniform in thickness, crack-free, have high mechanical density, reproducibility, and good piezoelectric performance. Reproducibility and good piezoelectric performance can be achieved by formulating optimised paste composition. The curing or co-firing temperature is crucial to determining the piezoelectric properties of the films, while screen-printing with correct pressure and snap-gap can control the film thickness and uniformity. The screen mesh and emulsion thickness are also important for controlling the film resolution and ensuring high quality prints.

The typical thickness of thick-films PZT ranges from a few microns to several hundred microns. The minimum film thickness is governed by the particle size of the PZT, which is typically 0.8 – 2  $\mu\text{m}$ . There is no theoretical upper limit of thickness that PZT film can be produced, but practically, films with thickness in excess of 200  $\mu\text{m}$  are generally inferior compared to bulk piezoelectric ceramics.

Thick-film PZT paste is made up of PZT powder as the functional component, a suitable permanent binding agent (such as lead borosilicate glass) and an organic vehicle (such as terpineol) which gives the paste its printable properties. Studies by Morten and co-workers [18] showed that the lower the glass content (about 3% by weight), the higher the value of piezoelectric charge coefficients. The type of permanent binder also influences the value of piezoelectric charge coefficients. It was reported that lead oxide was a better binder than lead alumina silicate glass.

It is also important to have the ability to control the electrical and mechanical performance of the thick films. Work on optimization of thick film PZT is described by Torah [19], who showed that the ball milled powders with larger particle size were able to produce higher piezoelectric activity. This can be further improved by combining ball and attritor milled particles to create high density films. A combination of 18 % attritor, 72% ball milled PZT powders, and 10% lead borosilicate glass (by weight) is the optimum paste composition. The experiments also showed that using a firing temperature of 1000<sup>0</sup>C, followed by poling with 4 MV/m electric field at 200<sup>0</sup>C produced a measured  $d_{33}$  value of 131 pC/N.

The first reported piezoelectric micro-generator based on thick-film technology is described by White *et al* [17]. It was printed on stainless steel and was able to generate power of 2  $\mu\text{W}$  at 80 Hz at 0.9 mm amplitude displacement (227.39  $\text{m/s}^2$ ). Thick-film materials printed onto substrates, however, are rigidly clamped on the surface and hence affect the piezoelectric materials' performance. To eliminate this problem, a better solution is to fabricate a free-standing structure, where the material can move freely under the influence of an ambient vibration source.

## 5. Free-Standing Structures

A free-standing (or free-supporting) structure is defined as one that stands alone, or on its own foundation, free of external support or attachment. These structures can be of variety of forms, from simple cantilevers to complex combination structures like honeycombs as shown in Fig.5.

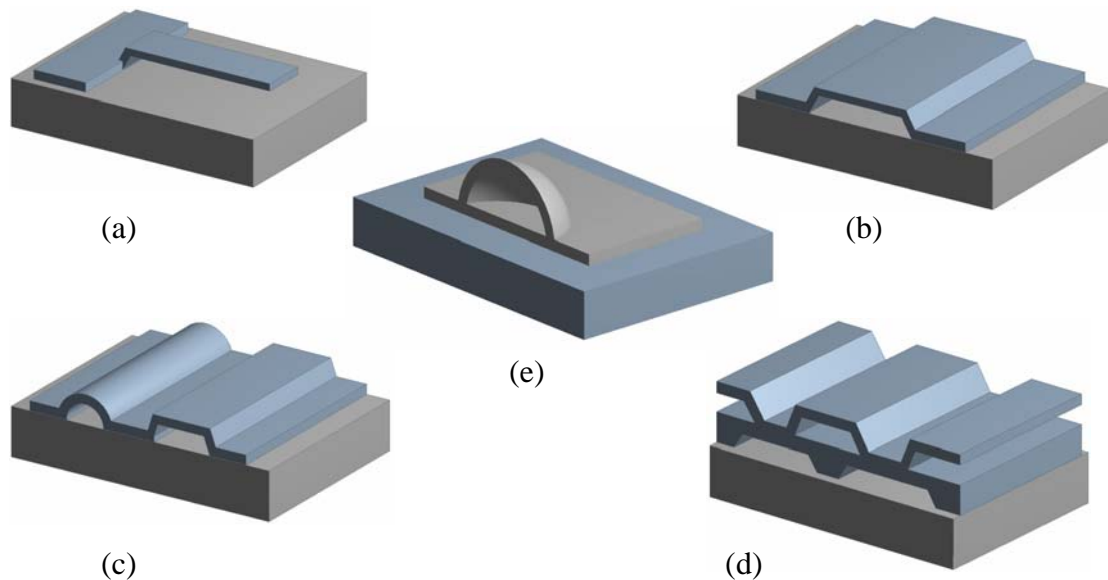


Fig.5. Free-standing micromechanical structure [20]: a) Cantilever, b) Bridge, c) Tunnel, d) Honeycomb, and e) Dome.

The wide acceptance for the integration of microelectronics and micromechanical systems (MEMS), has been one of the main drivers leading to the requirements free-standing micromechanical devices. The free-standing structures can be fabricated from smart materials (such as piezoelectrics), and hence they are often thought of as ‘intelligent’ structures that are able to sense and react to their environment [21]. With these capabilities, they can be used in a variety of applications, such as sensors, actuators and micro-generators for wireless sensor networks.

Some of the enabling technologies for fabricating free-standing intelligent structures include thick film, thin film, and silicon micromachining [22]. Recently, polymer technologies are also becoming popular, as reported in [23]. Some other techniques being reported for fabricating simple cantilever structures include the use of lasers [24], flip and bond methods [25], and electrostatic layer-by-layer techniques [26].

The remainder of this paper describes how thick-film technology can be adopted for the manufacture of free-standing piezoelectric structures. In order to create a free-standing structure, the active layers, which will become the moving structures, have to be deposited on rigid platforms. The platforms will then be removed usually by etching the material away in an appropriate manner. The platforms are called ‘sacrificial layers’, since they are eventually eliminated to release the materials deposited above them.

This technique is not new, as it is often used in surface micromachining, where a silicon substrate is selectively etched to produce free-standing structures. The sacrificial layer for surface micromachining is usually either a silicon oxide, phosphosilicate glass or photoresist. Unfortunately, silicon surface micromachining can involve expensive, complex and time-consuming processes. Thick-film technology presents an alternative way to fabricate free-standing structures.

Early research on free-standing thick-film structures fabricated from cermet thick-films and printed onto alumina is described by Stecher [20] and Singh *et al* [27]. One difference from the etching techniques used in the thin-film and silicon technologies, is that the free-standing structure fabricated with thick-film technology is the residual structure of the sublimation of sacrificial layer at elevated temperatures. It does not require any chemicals to remove the sacrificial layer. This obviously is another potential advantage for thick-film technology in terms of its ability for environmentally friendly processing.

As reported in [20, 28], the fabrication method for free supporting structures, combines the processing of air and nitrogen-fireable materials on the same substrate. Firstly, a carbon-like filler is printed and fired on those areas of the substrate where the structure will be freely supported. The filler is used to prevent the following printed dielectric layer from being bonded to the substrate. The second step of the process requires a nitrogen-fireable dielectric material to be printed on top of the filler and parts of the substrate. The structure is then fired in a nitrogen atmosphere, which must be used because the filler must not burn out before the glass-ceramic has sintered. Finally, an air firing process is carried out, where the filler gets burnt out without leaving a residue, and hence a free-standing structure is produced.

Recent work at the University of Southampton has demonstrated the feasibility of producing thick-film free-standing structures using the carbon sacrificial layer technique. A few structures were fabricated with equal widths of 10 mm and thicknesses of 80  $\mu\text{m}$ , and varying lengths from 4.5 mm to 18 mm. They were poled at an electric field strength of 3 MV/m at 200 $^{\circ}\text{C}$  for 30 minutes. The purpose of this work was to explore the possibility of producing thick-film piezoceramic free-standing structures to function as micro-generators. Fig.6a and Fig.6b shows photograph images of free-standing cantilevers with plate electrodes and interdigitated electrodes respectively.

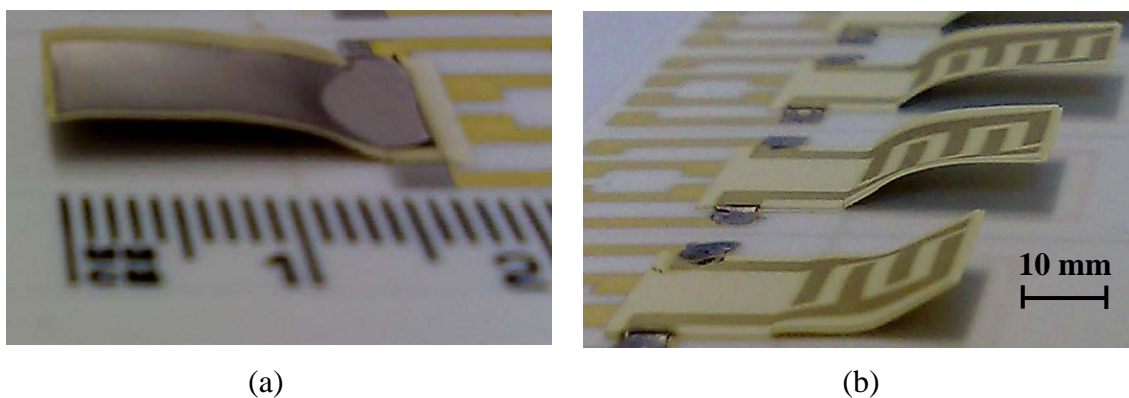


Fig.6. (a) Free-standing structure of a cantilever covered with plate-type electrodes and having a length of 15 mm, rising from a fixed area on an alumina substrate, (b) Free-standing structures of cantilevers covered with interdigitated electrodes of different lengths.

## 6. Measurement Results

A direct piezoelectric effect method was used to characterise the free-standing structures. The devices were vibrated with a shaker with different frequencies and acceleration levels. Proof masses and electrical load resistances were used to study the optimum output, in term of voltage and power, and their influence on the natural frequency of the piezoceramic free-standing structures.

Measurement results show that resonance frequency reduced as the length of cantilevers increased, which is as expected as in equation (3) and in agreement with the simulation results as shown in Fig.7. The open circuit voltage produced by the microgenerator increases proportionally with the length of the cantilever. When an optimum electrical load resistance is applied to the circuit, the voltage was seen to drop as shown in Fig.8. A cantilever of length 18 mm produces an open circuit voltage of 130 mV, while with added load resistance the voltage across it is dropped to 20 mV. This, of course, does not necessarily mean that the output power is reduced accordingly (at open circuit, the load resistance tends towards infinity). Fig.9 shows a selection of plots (for beams of differing length) that demonstrate how the output power varies with load resistance. There is clearly a specific value of load resistance that provides the maximum power. The power output can be further increased by exciting the structure at a higher input acceleration level (and obeys a square law relationship). A problem, as illustrated in Fig.10, is that a nonlinear frequency response is observed and this can result in the structure not producing maximum power output, despite being connected to an optimum load resistance.

The performance of a free-standing micro-generator is also dependent on the size of the proof mass attached at the tip of the cantilever. The proof mass can be used to adjust the natural frequency of the cantilever to match the ambient vibration sources. As shown in Fig.11, a cantilever with an added mass reduces the natural frequency by a factor of five when compared to one without the additional mass. The effect of the added mass on power output is shown in Fig.12.

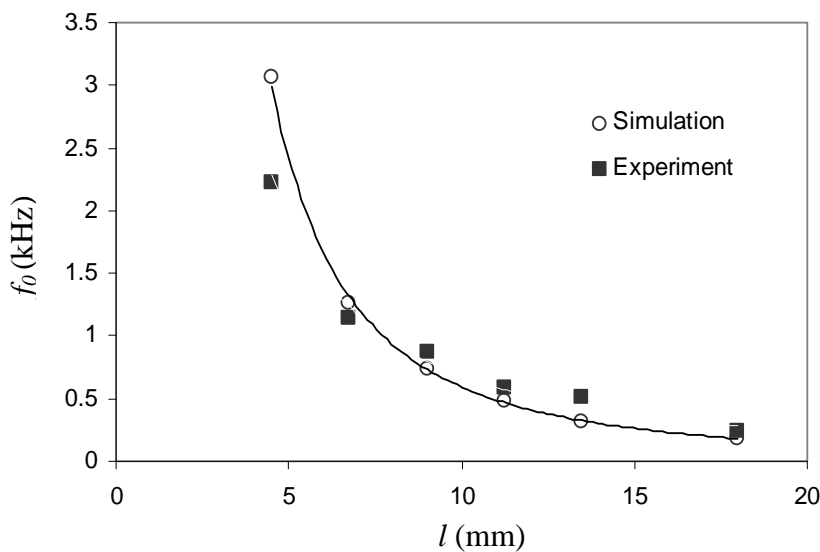


Fig.7. The natural frequency of a free-standing structure is inversely proportional to the length of the structure.

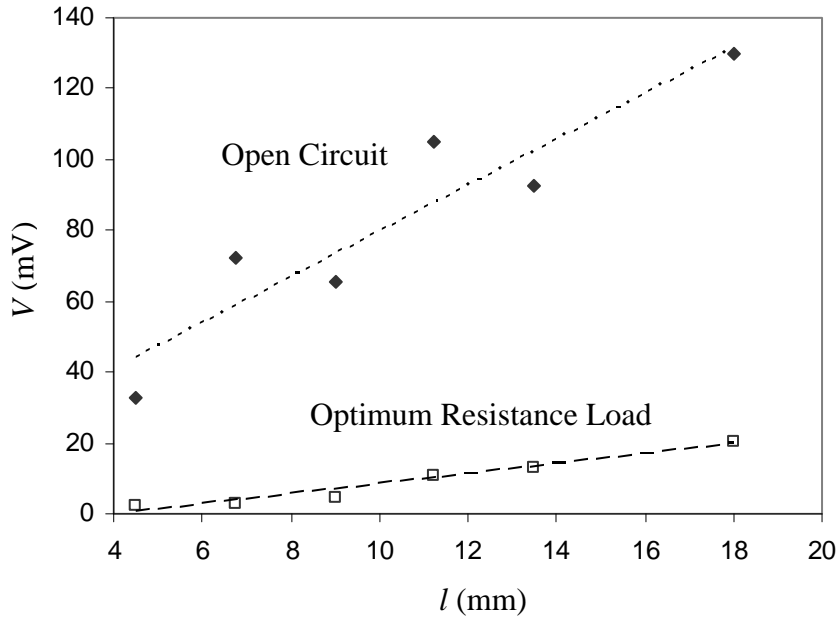


Fig.8. Comparison between voltage across optimum resistance load and open circuit voltage for various lengths of cantilever, vibrated at an acceleration of  $1 \text{ m/s}^2$ .

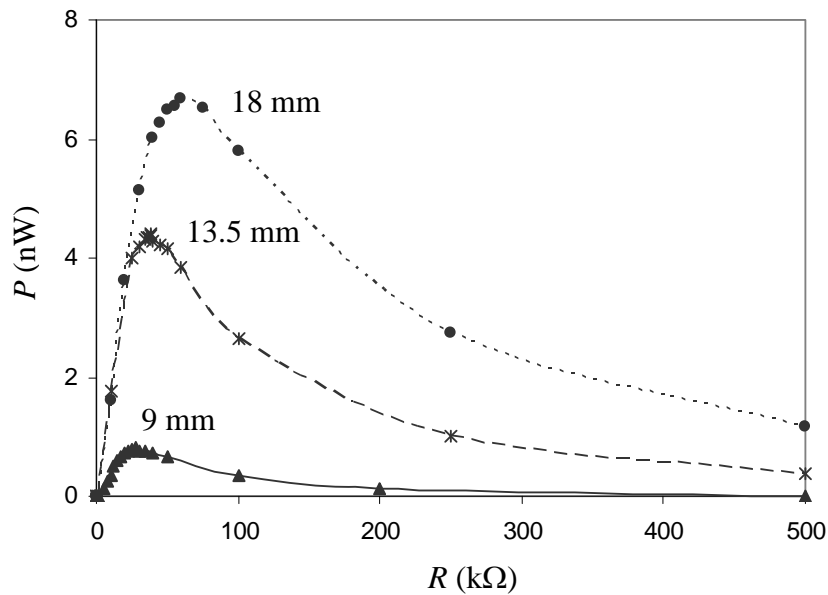


Fig.9. Maximum power output at matching load resistance for cantilever with length 9 mm, 13.5 mm, and 18 mm, and vibrated at acceleration of  $1 \text{ m/s}^2$ .

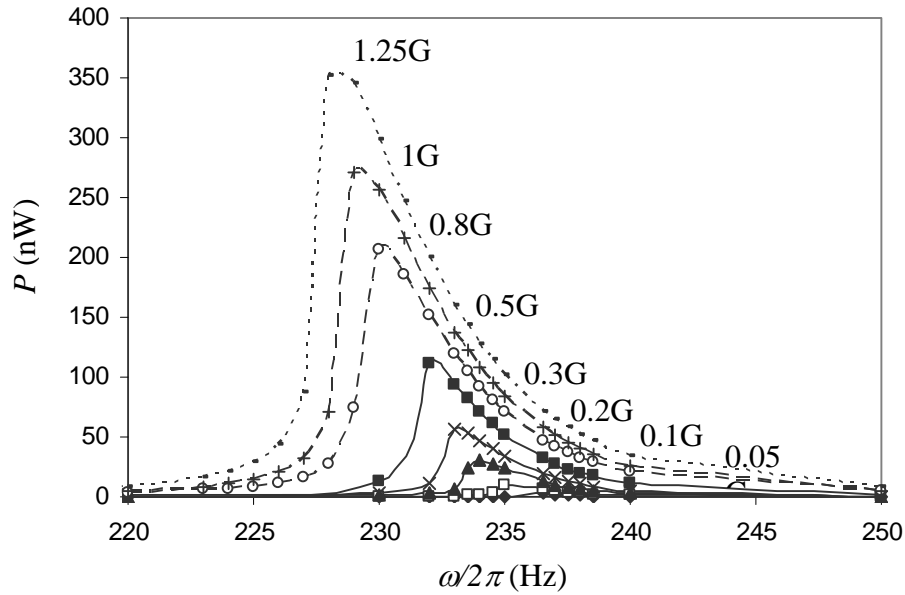


Fig.10. Frequency responds for a cantilever with length 18 mm, at difference acceleration levels (1G = 9.81 m/s<sup>2</sup>).

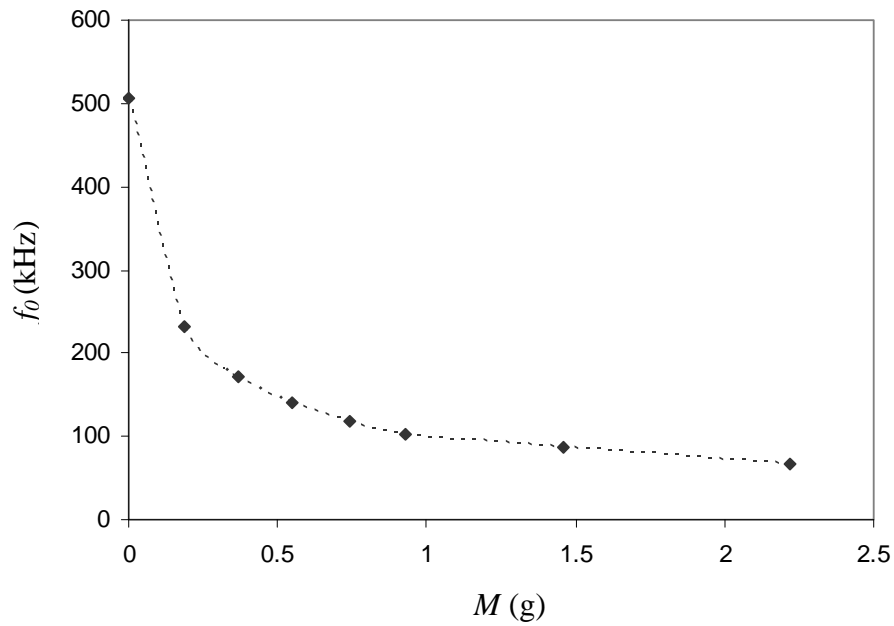


Fig.11. Natural frequency of a cantilever with length 13.5 mm, drops with proof mass  $M$  which attached at the tip of cantilever.

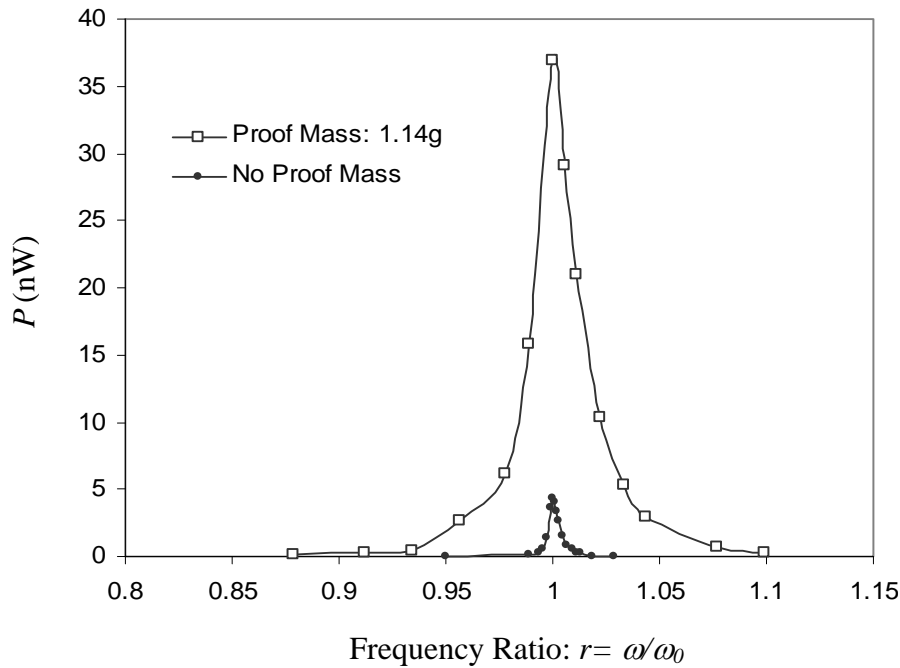


Fig.12. Power output increases about eight times as a proof mass of 1.14g is attached at the tip of a cantilever.

## 7. Conclusions

For the production of a compact energy sources for embedded systems applications such as sensor nodes, a piezoelectric micro-generator provides a good choice for generating a sustained level of electrical energy harvested from an ambient vibration environment. Such vibration sources are usually low frequency ( $< 500$  Hz), and a robust and flexible free-standing structure can be used for this purpose. The performance of a free-standing structure fabricated with thick-film technology has been described. It was found to be capable of functioning at low level frequencies and can potentially be used with MEMS structures. Additionally, thick-film devices are relatively low-cost and can be manufactured with mass production techniques. Future work is underway to design and fabricate optimum thick-film piezoceramic micro-generators, which are capable of powering various types of micro-electronic device.

## 8. References

- [1] Merhaut J. Theory of Electroacoustics. McGraw-Hill, New York.; 1981.
- [2] Williams CB, Yates RB. Analysis of a micro-electric generator for microsystems. *Transducers 95/Eurosensors IX* 1995;369-72.
- [3] Anton SR, Sodano HA. A review of power harvesting using piezoelectric materials (2003&ndash;2006). *Smart Materials and Structures* 2007;16(3):R1-R21.
- [4] Roundy S, Wright PK. A piezoelectric vibration based generator for wireless electronics. *Smart Materials and Structures*, IOP 2004;12:1131-42.
- [5] Polla DL, Francis LF. Processing and characterization of piezoelectric materials and integration into microelectromechanical systems. *Annual Review of Materials Science* 1998 Aug;28:563-97.
- [6] Jordan TL, Ounaies Z. Piezoelectric Ceramics Characterization. NASA/CR-2001-211225 ICASE Report, No. 2001-28; 2001.
- [7] High Quality Components and Materials for The Electronic Industry. Ferroperm Piezoceramics; 2003 May.
- [8] Piezoelectric ceramics data book for designers. Morgan Electroceramics; 1999.
- [9] Kaajakari V, Rodgers S, Lal A. Ultrasonically driven surface micromachined motor. *Proc 3rd IEEE Conf MicroElectroMechanical Systems* 2000;40-5.
- [10] Ueberschlag P. PVDF piezoelectric polymer. *Sensor Review* 2001 Apr 25;21:118-26.
- [11] Harrison JS, Ounaies Z. Piezoelectric Polymers. NASA/CR-2001-211422 ICASE Report, No. 2001-43; 2001.
- [12] Jeon YB, Sood R, Jeong J, Kim S-G. MEMS Power Generator with Transverse Mode Thin Film PZT. *Sensor and Actuators A* 2005;(122):16-22.
- [13] Larry JR, Rosenberg RM, Uhler RO. Thick-film technology: an introduction to the materials. *IEEE Trans on Components, Hybrids, and Manufacturing Technology* 1980;CHMT-3(3):211-25.
- [14] Brignell JE, White NM, Cranny AWJ. Sensor applications of thick-film technology. *Communications, Speech and Vision, IEE Proceedings I* 1988;135(4):77-84.
- [15] White NM, Brignell JE. A planar thick-film load cell. *Sensors and Actuators* 1991;25 - 27:313-9.
- [16] Arshak KI, Ansari F, McDonagh D, Collins D. Development of a novel thick-film strain gauge sensor system. *Measurement Science and Technology* 1997;8(1):58-70.
- [17] White NM, Glynne-Jones P, Beeby SP. A novel thick-film piezoelectric micro-generator. *Smart Mater Struct* 2001;10:850-2.
- [18] Torah RN, Beeby SP, Tudor MJ, White NM. Thick-film piezoceramics and devices. *J Electroceram* 2007;19:95-110.
- [19] Torah RN, Beeby SP, White NM. Improving The Piezoelectric Properties of Thick-Film PZT: The Influence of Paste Composition, Powder Milling Process and Electrode Material. *Sensor and Actuators A* 2004;110:378-84.
- [20] Stecher G. Free Supporting Structures in Thick-Film Technology: A Substrate Integrated Pressure Sensor. 6th European Microelectronics Conferences, Bournemouth 1987;421-7.

- [21] Seeley CE, Chattopadhyay A. The development of an optimization procedure for the design of intelligent structures. *Smart Materials and Structures* 1993;2(3):135-46.
- [22] Yalcinkaya F, Powner ET. Intelligent Structures. *Sensor Review* 1996;16:32-7.
- [23] Fu Y, Harvey EC, Ghantasala MK, Spinks GM. Design, fabrication and testing of piezoelectric polymer PVDF microactuators. *Smart Materials and Structures* 2006;15(1):S141-S146.
- [24] Allard M, Boughaba S, Meunier M. Laser micromachining of free-standing structures in SiO<sub>2</sub>-covered silicon. *Applied Surface Science* 1997 Feb 1;109-110:189-93.
- [25] Papakostas T. Polymer Thick-Film Sensor and Their Integration with Silicon: A Route to Hybrid Microsystems. PhD Thesis, University of Southampton, November; 2000.
- [26] Cadd D, Cadd D, Wood D, Petty MC. Free-standing polymer cantilevers and bridges reinforced with carbon nanotubes  
Free-standing polymer cantilevers and bridges reinforced with carbon nanotubes. *Micro & Nano Letters, IET* 2007;2(3):54-7.
- [27] Singh A, Prudenziati M, Morten B. Technique for lifting off thick film print fired on alumina. *Microelectronics Reliability* 1985;25:619-20.
- [28] Birol H, Maeder T, Ryser P. Fabrication of LTCC Micro-fluidic Devices Using Sacrificial Carbon Layers. *J Appl Ceram Technol* 2005;2:345-54.